Polarization dynamics in a vertical-cavity laser with an axial magnetic field

C. Serrat,[1,2,*] N. B. Abraham,[1,3,†] M. San Miguel,[3] R. Vilaseca,[2] and J. Martín-Regalado[3]
[1]*Department of Physics, Bryn Mawr College, 101 North Merion Avenue, Bryn Mawr, Pennsylvania 19010-2899*
[2]*Departament de Física i Enginyeria Nuclear, Universitat Politècnica de Catalunya, Colom 11, E-08222 Terrassa, Spain*
[3]*Departament de Física, Universitat de les Illes Balears (UIB) and Instituto Mediterraneo de Estudios Avanzados (IMEDEA), Consejo Superior de Investigaciones Científicas, E-07071 Palma de Mallorca, Spain*
(Received 20 February 1996)

An axial magnetic field applied to vertical-cavity surface-emitting lasers induces emission of elliptically polarized states. The characteristic switching between orthogonal linearly polarized states with no magnetic field becomes a switching between elliptically polarized states with low ellipticity for weak magnetic fields. Stronger magnetic fields induce time-dependent solutions with two main peaks in the optical spectrum, with orthogonal elliptically polarized basis states. Strong magnetic fields induce rotating linearly polarized emission. [S1050-2947(96)50606-2]

PACS number(s): 42.55.Px, 42.60.Mi, 42.65.Sf, 42.55.Sa

Vertical-cavity, surface-emitting lasers (VCSELs) most often emit linearly polarized light preferentially oriented along one of two perpendicular directions associated with the crystal axes. These two polarization modes have different optical frequencies split, typically by a few GHz, by the material birefringence. For relatively low injection currents, VCSELs commonly emit in the fundamental transverse mode, with a relatively abrupt switch between the states of linear polarization as the injection current is increased [1–5].

This general phenomenology is also found within a theoretical framework [6], based on a model [7] that incorporates the vector nature of the electric field, saturable dispersion associated with the linewidth enhancement factor (or antiguiding parameter) of semiconductors, and carrier dynamics associated with the different magnetic sublevels of the conduction and heavy-hole valence bands.

In addition to the linearly polarized states the analysis [6,8,9] predicts elliptically polarized states (and states of temporally modulated ellipticity) as intermediates in the switching between the linearly polarized states. Long-lived, but weakly unstable ''two-frequency solutions'' have also been found in the model [10], for which the total field spectrum shows two frequencies with roughly the same amplitude and with each spectral component corresponding to a different state of polarization. These features persist when the Gaussian profile of the mode is included [10].

Elliptically polarized emission was observed experimentally for VCSELs in an axial magnetic field [11], with greater ellipticity close to the lasing threshold and for larger magnetic fields. A small remnant ellipticity was also observed at zero magnetic field.

From the point of view of a model for VCSELs such as [6,7], one would expect an applied magnetic field to enhance the dynamical role of the magnetic sublevels by breaking the degeneracy of the resonant frequencies for left and right circularly polarized fields interacting with different magnetic sublevels. When combined with the intrinsic birefringence of the VCSEL, the magnetically induced Faraday effect would then naturally transform the preferred basis states of the system from linearly polarized states to elliptically polarized states. An extreme case of magnetically decoupled radiation channels for nondegenerate transitions for circularly polarized fields might lead to simultaneous emission on both transitions, with the frequency difference resulting in a state of rotating linear polarization. This leads us to expect that a magnetic field of intermediate strength might stabilize two-frequency solutions with simultaneous emission of two elliptically polarized states. The remnant ellipticity observed experimentally for zero applied field may be a result of stray fields or an indication of some material process that breaks the sublevel degeneracy.

Motivated by these expectations we analyze in this paper the predictions of the general theoretical framework of [6,7] for VCSELs with an axial magnetic field based in the model given by [6]

$$\frac{dE_{\pm}}{dt} = -\kappa E_{\pm} - i\omega_0 E_{\pm} + \kappa(1+i\alpha)(N\pm n)E_{\pm} - i\gamma_p E_{\mp} - \gamma_a E_{\mp} \pm i\gamma_z E_{\pm} \pm \gamma_c E_{\pm}, \quad (1)$$

$$\frac{dN}{dt} = -\gamma(N-\mu) - \gamma(N+n)|E_+|^2 - \gamma(N-n)|E_-|^2, \quad (2)$$

$$\frac{dn}{dt} = -\gamma_s n - \gamma(N+n)|E_+|^2 + \gamma(N-n)|E_-|^2, \quad (3)$$

where $E_{\pm}$ are the slowly varying, complex amplitudes of the circularly polarized components of the vector electric field. N is the total population difference between the conduction and valence bands; μ is the normalized injection current; n is the difference in the population differences on the two allowed transitions between magnetic sublevels; α is the linewidth enhancement factor; $\omega_0 = \kappa\alpha$ is a frequency shift for the slowly varying amplitudes that leads to a zero optical frequency at the lasing threshold in the absence of phase

*Electronic address: serrat@fen.upc.es
†Electronic address: nabraham@brynmawr.edu

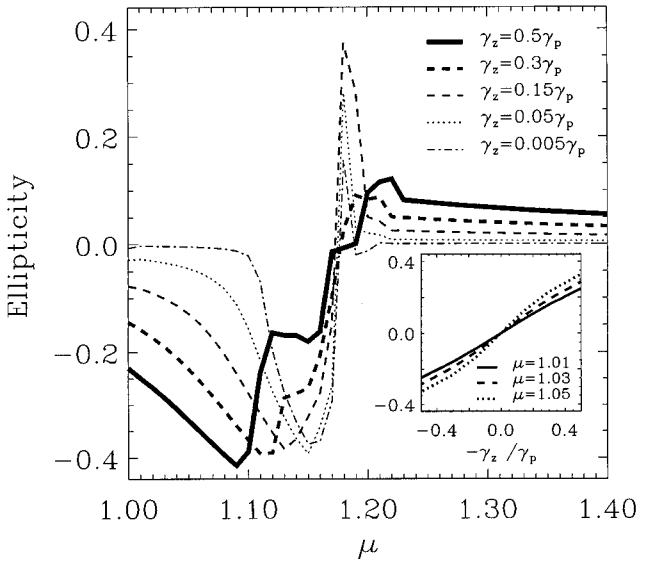

FIG. 1. Ellipticity (χ) vs injection current (μ) for indicated values of magnetic field strength (γ_z). Inset: χ vs γ_z for small values of μ.

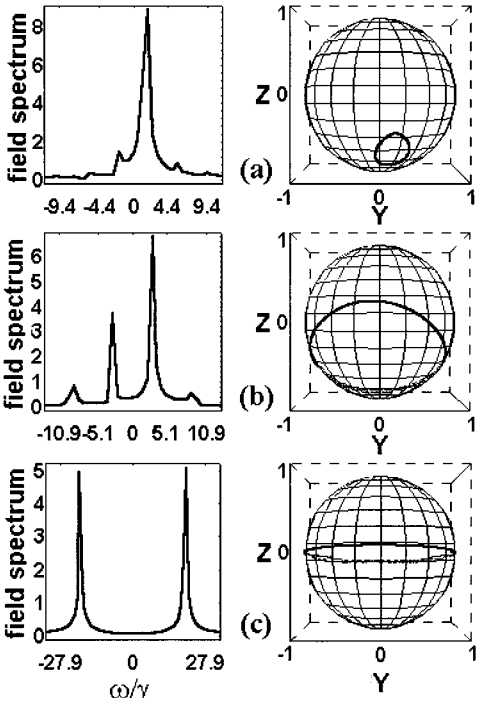

FIG. 2. Optical power spectrum and Poincaré sphere representation of time-dependent solutions termed (a) M, (b) R, and (c) R_L as discussed in the text. Parameters: (a) $\mu=1.16$, $\gamma_z=0.01\gamma_p$; (b) $\mu=1.1$, $\gamma_z=\gamma_p$; (c) $\mu=1.1$, $\gamma_z=10\gamma_p$.

anisotropies; γ_p represents the effect of birefringence; γ_a and γ_c are the strengths of the anisotropic amplitude losses for the linearly and circularly polarized modes, respectively; and γ_z represents the magnetic-field-induced frequency splitting of the circularly polarized modes in the absence of other anisotropies.

When there is no magnetic field and no circular anisotropies ($\gamma_z=\gamma_c=0$) these equations predict different domains of stability for the x- and y-polarized steady (constant-intensity) states [6,10], which have different optical frequencies given by $+\gamma_p$ and $-\gamma_p$, respectively. Depending on the values of the birefringence parameter γ_p and the injection current μ, either one, both, or none of the two linearly polarized states are stable. As an illustration we restrict this paper to a situation of low birefringence ($\gamma_p=2\gamma$) with $\gamma_c=0$ in which increasing μ changes the system from a domain of bistability to a domain in which only y-polarized emission is stable. Other chosen parameter values are $\kappa=300\ \mathrm{ns}^{-1}$, $\gamma=1\ \mathrm{ns}^{-1}$, $\gamma_s=50\ \mathrm{ns}^{-1}$, $\alpha=3$, and $\gamma_a=-0.1$. With the small negative value for the amplitude anisotropy (γ_a) x-polarized emission is favored close to threshold and there is a switch from x- to y-polarized emission at approximately $\mu=1.15$.

With nonzero magnetic field the steady states are elliptically polarized (with small ellipticity when the magnetic field is weak) with their azimuths tilted towards the x and y axes, denoted by ϵ_x and ϵ_y, respectively. These can be characterized by an ellipticity parameter defined as

$$\chi(t)=\frac{1}{2}\arcsin\left(\frac{|E_+(t)|^2-|E_-(t)|^2}{|E_+(t)|^2+|E_-(t)|^2}\right). \tag{4}$$

Figure 1 shows the ellipticity for the solution found as the injection current was increased in small steps. The inset shows that, for μ below the polarization switching point, χ increases with both increasing μ and increasing γ_z, in accord with the experimental observations [11]. For μ values above the polarization switch χ decreases with further increases in μ.

With increasing magnetic field, time-dependent solutions are more prevalent. Three qualitatively different time-dependent states have two predominant peaks in their optical spectra. Samples are presented in Fig. 2. We denote them as M (elliptical polarization with modulated ellipticity and modulated azimuth about nonzero mean values), R (states with periodically modulated ellipticity around a zero mean and with a rotating azimuth), and R_L (rotating linearly polarized emission). Their characterization in Fig. 2 is given in terms of their total field spectrum (sum of the power spectra of E_- and E_+) and their representation in the Poincaré sphere [12].

The state we call M has unequal strengths in its spectral components, elliptical polarization for each spectral component, and a small closed trajectory on the Poincaré sphere. The stronger spectral component has the elliptical polarization state given by the center of the trajectory. The state we call R has two nearly equally strong spectral components, and is thus represented by what is nearly a great circle on the Poincaré sphere. The elliptically polarized states of the spectral components are given by the intersections of the surface of the Poincaré sphere with the diameter which is perpendicular to the plane of the circular trajectory. R_L is a limiting case of R in which the basis states of the spectral components are circularly polarized, a condition reached only asymptotically for large magnetic fields for the parameters we have chosen. The state that is nearly R_L, which is shown in Fig. 2(c), has a small residual modulation of the ellipticity.

The time-dependent states are found as intermediate states in the switching from ϵ_x to ϵ_y with adiabatically increasing

	$100\gamma_p$	C_-	R_L	R_L	R_L	R_L	R_L	R_L	$\cdots$	R_L
	$10\gamma_p$	C_-	R_L	R_L	R_L	R_L	R_L	R_L	$\cdots$	R_L
	γ_p	ϵ_x	R	R	R	R	R	ϵ_y	$\cdots$	ϵ_y
γ_z	$0.7\gamma_p$	ϵ_x	M	R	R	R	ϵ_y	ϵ_y	$\cdots$	ϵ_y
	$0.1\gamma_p$	ϵ_x	ϵ_x	ϵ_x	M	R	ϵ_y	ϵ_y	$\cdots$	ϵ_y
	$0.01\gamma_p$	ϵ_x	ϵ_x	ϵ_x	ϵ_x	R	ϵ_y	ϵ_y	$\cdots$	ϵ_y
	0	L_x	L_x	L_x	ϵ_x	R	L_y	L_y	$\cdots$	L_y
(a)	μ	1.0	1.05	1.10	1.15	1.20	1.25	1.30	$\cdots$	2.0

	$100\gamma_p$	R_L	R_L	R_L	R_L	R_L	R_L	R_L	$\cdots$	R_L
	$10\gamma_p$	R_L	R_L	R_L	R_L	R_L	R_L	R_L	$\cdots$	R_L
	γ_p	ϵ_x	R	R	R	ϵ_y	ϵ_y	ϵ_y	$\cdots$	ϵ_y
γ_z	$0.7\gamma_p$	ϵ_x	M	R	ϵ_y	ϵ_y	ϵ_y	ϵ_y	$\cdots$	ϵ_y
	$0.1\gamma_p$	ϵ_x	ϵ_y	ϵ_y	ϵ_y	ϵ_y	ϵ_y	ϵ_y	$\cdots$	ϵ_y
	$0.01\gamma_p$	ϵ_x	ϵ_y	ϵ_y	ϵ_y	ϵ_y	ϵ_y	ϵ_y	$\cdots$	ϵ_y
	0	L_x	L_y	L_y	L_y	L_y	L_y	L_y	$\cdots$	L_y
(b)	μ	1.0	1.05	1.10	1.15	1.20	1.25	1.30	$\cdots$	2.0

FIG. 3. Sequence of states (L—linear polarized, others as identified in Fig. 2 and the text) observed with adiabatically (a) increased and (b) decreased injection current for indicated γ_z. M—states always appeared with increasing μ between ϵ_x and R states, but they are not indicated unless they appeared for the specific values of μ chosen for the tables.

current, as indicated in the phase diagram shown in Fig. 3(a) for the control parameters μ and γ_z. For simplicity we use the symbol M in this figure to denote not only the time-dependent states of modulated ellipticity, such as that shown in Fig. 2(a) (which appears after a Hopf bifurcation destabilizes the ϵ_x solution), but also more complicated states of modulated ellipticity including figure-8's on the Poincaré sphere. The results for no magnetic field include states labeled L_x and L_y for x- and y-polarized states, respectively.

We find three different scenarios in this switching process, depending on the strength of the magnetic field (γ_z). (1) For a weak magnetic field ($\gamma_z \ll \gamma_p$) the switching from ϵ_x to ϵ_y occurs through narrow regions of intermediate M and R states. This is a small modification of what happens for zero magnetic field where the switch from L_x to L_y occurs through intermediate ϵ_x and M states. (2) When $\gamma_z \sim \gamma_p$, the switching occurs through broader regions of intermediate M and R states. (3) For very large magnetic fields, the state selected close to threshold is nearly circularly polarized (in this case C_-) and it switches to an R state as the injection current is increased. The instantaneous ellipticity of these R states becomes very small with strong magnetic fields and asymptotically they become R_L states.

For low injection current the system is bistable; hence there is hysteresis if the injection current is first raised from the lasing threshold to a value greater than 2 and then lowered, with the switching that occurs as μ is decreased [Fig. 3(b)] appearing at a lower value of the μ.

These results indicate that substantial zones of polarization switching that may be useful for signaling applications remain for low magnetic fields, with the switching occurring between distinguishable states of different azimuth and low ellipticity. The dynamically significant strength of magnetic fields for qualitative changes in behavior is set by $\gamma_z \sim \gamma_p$.

Note added in proof. Recently we learned of related theoretical work [13] extending, as here, the theory [6–10] to include magnetic fields and circular loss anisotropies. They provide analytical solutions for the elliptically polarized states.

We are grateful for helpful discussions of these problems with F. Prati, G. Tissoni, J.P. Woerdman, M. Van Exter, M. Travagnin, and H. Li. C.S. and R.V. acknowledge support from the Spanish Dirección General de Investigación Científica y Técnica (Contract No. PB92-0660-C03). M.S.M. and J.M.R. acknowledge financial support from the Comisión Interministerial de Ciencia y Tecnología, Project Nos. PB94-1167 and TIC95/0563, and European Union HCM Grant No. CHRX-CT-94-0594.

[1] C.J. Chang-Hasnain, J.P. Harbison, G. Hasain, A.C. Von Lehmen, L.T. Florez, and N.G. Stoffel, IEEE J. Quantum Electron. **27**, 1402 (1991).

[2] K.D. Choquette and R.E. Leibenguth, IEEE Photonics Technol. Lett. **6**, 40 (1994).

[3] K.D. Choquette, D.A. Richie, and R.E. Leibenguth, Appl. Phys. Lett. **64**, 2062 (1994).

[4] J. McInerney *et al.*, Chaos, Solitons Fractals **4**, 1619 (1994).

[5] Z.G. Pan, S. Jiang, and M. Dagenais, Appl. Phys. Lett. **63**, 2999 (1993).

[6] J. Martin-Regalado, M. San Miguel, N.B. Abraham, and F. Prati, Opt. Lett. **21**, 351 (1996).

[7] M. San Miguel, Q. Feng, and J.V. Moloney, Phys. Rev. A **52**, 1728 (1995).

[8] J. Martin-Regalado, N.B. Abraham, M. San Miguel, F. Prati, and G. Tissoni, in *Nonlinear Dynamics in Laser Systems*, edited by N.B. Abraham and Ya.I. Khanin, SPIE Proc. Vol. 2792 (SPIE, Bellingham, WA, in press).

[9] J. Martin-Regalado, M. San Miguel, N.B. Abraham, and F. Prati, in *Physics and Simulation of Optoelectronic Devices IV*, edited by W.W. Chow and M. Osinski, SPIE Proc. Vol. 2693 (SPIE, Bellingham, WA, 1996).

[10] J. Martin-Regalado, F. Prati, M. San Miguel, and N.B. Abraham, IEEE J. Quantum Electron. (to be published).

[11] M.P. van Exter (unpublished); A.K. Jansen van Doorn, M.P. van Exter, M. Travagnin, and J.P. Woerdman (unpublished); M.P. van Exter, A.K. Jansen van Doorn, and J.P. Woerdman, in *Physics and Simulation of Optoelectronic Devices IV* (Ref. [9]).

[12] H. de Lang, D. Polder, and W. van Haeringen, Philips Tech. Rev. **32**, 190 (1971).

[13] M. Travagnin, M.P. van Exter, A.K. Jansen van Doorn, and J.P. Woerdman, Phys. Rev. A (to be published).